THE JOURNAL OF BIOLOGICAL CHEMISTRY VOL. 284, NO. 26, pp. 17607–17615, June 26, 2009

Smooth Muscle Archvillin Is an ERK Scaffolding Protein*

Received for publication, April 1, 2009, and in revised form, April 27, 2009 Published, JBC Papers in Press, April 29, 2009, DOI 10.1074/jbc.M109.002386

Samudra S. Gangopadhyay[‡§1], Edouard Kengni[‡1], Sarah Appel[‡1], Cynthia Gallant[‡§], Hak Rim Kim[‡], Paul Leavis[§¶], Jon DeGnore[¶], and Kathleen G. Morgan[‡§2]

From [‡]Boston University, Boston, Massachusetts 02215, the [§]Boston Biomedical Research Institute, Watertown, Massachusetts 02472, and the [¶]Tufts University School of Medicine, Boston, Massachusetts 02111

ERK influences a number of pathways in all cells, but how ERK activities are segregated between different pathways has not been entirely clear. Using immunoprecipitation and pulldown experiments with domain-specific recombinant fragments, we show that smooth muscle archvillin (SmAV) binds ERK and members of the ERK signaling cascade in a domain-specific, stimulus-dependent, and pathway-specific manner. MEK binds specifically to the first 445 residues of SmAV. B-Raf, an upstream regulator of MEK, constitutively interacts with residues 1–445 and 446–1250. Both ERK and 14-3-3 bind to both fragments, but in a stimulus-specific manner. Phosphorylated ERK is associated only with residues 1–445. An ERK phosphorylation site was determined by mass spectrometry to reside at Ser[132]. A phospho-antibody raised to this site shows that the site is phosphorylated during α-agonist-mediated ERK activation in smooth muscle tissue. Phosphorylation of SmAV by ERK decreases the association of phospho-ERK with SmAV. These results, combined with previous observations, indicate that SmAV serves as a new ERK scaffolding protein and provide a mechanism for regulation of ERK binding, activation, and release from the signaling complex.

The ERK[3] cascade has long been known to be central to the activation of cellular processes such as proliferation, differentiation, and oncogenic transformation (1). More recently, it has become clear that this cascade also plays a major role in the regulation of motility and contractility (2–4). The MAPK serine/threonine family of protein kinases, of which ERK is a member, are evolutionarily conserved and are activated by a mechanism that includes protein kinase cascades. Original studies performed with *Saccharomyces cerevisiae* have demonstrated the importance of scaffold proteins in providing coordination and specificity of the MAPK cascades. The yeast protein Ste5 is a critical regulator of the mating response in yeast because of its ability to act as a scaffold to assemble the MAPK kinase kinase homolog Ste11 and the MEK homolog Ste7 to activate the MAPK, Fus3. No mammalian protein shares significant similarity at the sequence level to Ste5 (2), but several mammalian proteins have been shown to exert scaffolding functions for parts of the MAPK activation cascades. Of note, with respect to ERK activation, are β-arrestin-1,2, which binds to Raf-1, MEK1, and ERK2; KSR, which associates with Raf, MEK1/2, ERK1/2, and 14-3-3; MEKK1, which associates with Raf-1, MEK1, and ERK2; and MP1, which binds to MEK1, ERK1, and p14 (5, 6).

We have previously reported the identification, in smooth muscle tissue, of a new splice variant of the supervillin family, smooth muscle archvillin (SmAV) (7) that is co-targeted to the cell cortex with ERK during α-agonist activation. Antisense knockdown of SmAV was shown to inhibit ERK activation, and it was postulated that ERK might form a macromolecular complex with SmAV to regulate its signaling function. In the present study we directly demonstrate the agonist- and pathway-specific formation of a complex containing SmAV and members of the ERK signaling module, MEK, B-Raf, and 14-3-3 both *in vitro* and *in vivo* in smooth muscle cells. Thus, SmAV functions as a pathway-specific scaffold to couple ERK activation in a spatially restricted manner to select outcomes.

EXPERIMENTAL PROCEDURES

Tissue Collection and Homogenization—Ferrets (Marshall Farms, North Rose, NY) were euthanized by an overdose of chloroform. Abdominal aortas were excised quickly to a dish containing oxygenated physiological saline solution (PSS; 120 mM NaCl, 5.9 mM KCl, 25 mM $NaHCO_3$, 11.5 mM dextrose, 2.5 mM $CaCl_2$, 1.2 mM $MgCl_2$, and 1.2 mM NaH_2PO_4, pH 7.4) as previously described (8). All of the procedures were approved by the Institutional Animal Care and Use Committee. For each ferret, three aorta tissue strips were prepared according to a method described by Menice *et al.* (9). Viability was tested by exposure to a solution where 51 mM KCl replaced an equimolar amount of NaCl (KCl PSS). The tissues were equilibrated for 1 h at 37 °C in oxygenated (95% O_2, 5% CO_2) PSS and then quick frozen in a dry ice/acetone/dithiothreitol slurry either without a stimulus or exposed to 10 μM phenylephrine for 4 min or 51 mM KCL PSS for 10 min. Both stimuli produce steady state maximal contraction of the tissue. For examining ERK-dependent SmAV phosphorylation, the tissues were pretreated either with 10 μM of the MEK inhibitor U0216 (Calbiochem, San Diego, CA) or Me_2SO, as a control, for 55 min before freezing in the presence of 10 μM phenylephrine for 4 min. The tissues were homogenized at 4 °C with a buffer containing 50 mM Tris-HCl, pH 7.4, 5 mM EGTA, 50 mM NaCl, 1.0% Nonidet P-40,

* This work was supported, in whole or in part, by National Institutes of Health Grants HL31704, HL80003, HL86655, and HD43054 (to K. G. M.) and HL074470 (to S. S. G.).

[1] These authors contributed equally to this work.

[2] To whom correspondence should be addressed: Boston University, 635 Commonwealth Ave., Boston, MA 02215. Fax: 617-353-7567; E-mail: kmorgan@bu.edu.

[3] The abbreviations used are: ERK, extracellular signal-regulated kinase; SmAV, smooth muscle archvillin; N-SmAV1, residues 1–445 of SmAV; N-SmAV2, residues 446–1250 of SmAV; MAPK, mitogen-activated protein kinase; PSS, physiological salt solution; PE, phenylephrine; MEK, MAPK/ERK kinase; DTT, dithiothreitol; IP, immunoprecipitation; Tricine, *N*-[2-hydroxy-1,1-bis(hydroxymethyl)ethyl]glycine; LC, liquid chromatography; MS/MS, tandem mass spectrometry.

1.0% sodium deoxycholate, 3 mM DTT, 67 μM $ZnCl_2$, 29.6 mM β-glycerophosphate, and protease inhibitors.

Generation of N-SmAV1 and N-SmAV2 Expression Plasmids—SmAV fragments were generated by PCR using ferret cDNA as template and the following primers: forward, 5′-ggt ggt tgc ggc cgc atg aaa aga aaa gaa aga att gcc cgg-3′; reverse for N-SmAV1, 5′-ggt ggt tgc ggc cgc tca gct ctc tgg ttc ctt ctg atg ttc cga agg-3′; and reverse for N-SmAV2, 5′-ggt ggt tgc ggc cgc ctg tca cac ccg cct ccc tct cag caa ctg-3′. The PCR products were cloned into the pTYB12 vector (NE Biolabs) using NotI restriction sites. The N-SmAV1-S132A mutant was generated with the XL site-directed mutagenesis kit (Stratagene) using primers forward 5′-ccg aag cgg act cgg aag cgc cgt ccc gat aca cc-3′ and reverse 5′-ggt gta tcg gga cgg cgc ttc cga gtc cgc ttc gg-3′.

Protein Expression—N-SmAV1 and N-SmAV2 (residues 1–445 and 446–1250 of SmAV, respectively). Intein-tagged protein fragments were expressed in *Escherichia coli* with an N-terminal chitin-binding domain tag (IMPACT-CN System NE Biolab). The methods were according to instructions of the supplier. Activated rat ERK2/constitutively activated MEK was expressed and purified according to Robbins *et al.* (10).

Pulldown Assay—Chitin-binding domain-tagged N-terminal fragments of SmAV were attached to affinity resins by passing expressed *E. coli* lysates through chitin beads. After several washes with a buffer containing 50 mM Tris-HCl, pH 7.5, 500 mM NaCl, and 1 mM EDTA, the resins were stored at 4 °C and used for pulldown assays. For the preparation of N-SmAV fragments without a tag, affinity resins were incubated with a buffer containing 20 mM Tris-HCl pH 8.0, 100 mM NaCl, 1 mM EDTA, and 100 mM DTT. The cleaved fragments were collected and dialyzed against phosphate-buffered saline to remove DTT. 200 μl of tissue homogenates were incubated overnight with 100 μl of affinity resin at 4 °C. The resins were subsequently washed three times with wash buffer containing 50 mM Tris-HCl, pH 7.4, 140 mM NaCl, 5 mM EGTA, 1.0% Nonidet P-40, 1.0% sodium deoxycholate, 3 mM DTT, 67 μM $ZnCl_2$, 29.6 mM β-glycerophosphate, and protease inhibitors. Bound partner proteins were eluted from the resin by boiling at 100 °C for 5 min with elution buffer (50 mM Tris-HCl, pH 6.8, 2% SDS, 10% glycerol, and protease inhibitors). Eluted proteins were detected by immunoblot with specific antibodies.

Immunoprecipitation (IP)—Tissue homogenates were precleared by incubating with a protein A-agarose slurry. Anti-MAPK/ERK1/2 (Millipore Upstate/Chemicon Biotech Inc., Billerica, MA) antibody, covalently bound to protein A-agarose beads, was mixed with each sample. As a negative control, tissue homogenates were incubated with normal rabbit IgG-agarose conjugate (Santa Cruz Biotechnology, Inc.). The mixture was incubated overnight at 4 °C with rocking. The beads were washed three times with 200 μl of fresh homogenization buffer and resuspended in a final volume of 80 μl. Immunoprecipitated proteins were extracted by boiling for 5 min. Immunoprecipitated proteins were detected by immunoblot with specific antibodies.

Antibodies—The mouse monoclonal p42/44 MAPK (1:1000 for immunoblot, 1:2000 for IP), rabbit polyclonal phospho-p44/42 MAPK (Thr^{202}/Tyr^{204}) (1:1000 for immunoblot, 1:2000 for IP), and rabbit polyclonal MEK1/2 antibodies (1:500) were from Cell Signaling Technology (Beverly, MA). The rabbit polyclonal B-Raf (H-145) (1:1000) antibody was from Santa Cruz Biotechnology, Inc. (Santa Cruz, CA). The monoclonal α-tubulin antibody (1:5000) and the supervillin antibody (1:1000) were from Sigma-Aldrich. The $Ser(P)^{132}$ SmAV antibody (see below) was used at a 1:500 dilution. The rabbit polyclonal 14-3-3 antibody, used at 1:500 dilution, was from Calbiochem. The rabbit polyclonal PAN-actin antibody (Cytoskeleton, Denver, CO) was used at 1:10000 dilution.

$Ser(P)^{132}$ SmAV Antibody—An octavalent multiple antigenic peptide (MAP) was synthesized (SEADSEpSPSRYTKSRK-DADA, corresponding to residues 126–145 of SmAV) using solid phase peptide synthesis on an Applied Biosystems model 433A peptide synthesizer with fluorenylmethoxycarbonyl (Fmoc) as the α-amino protecting group. MAP peptides are known to elicit strong antibody responses with higher titers compared with the monomeric peptide coupled to a carrier protein (11). A rabbit polyclonal antibody was raised against this phospho-MAP peptide by Capralogics. For affinity purification, an affinity column of the octavalent peptide was made using an Aminolink plus immobilization kit from Thermo Scientific (Rockford, IL), and the antibody was purified according to the instructions of the manufacturer. To assess the specificity of the phospho-antibody, SmAV peptides were separated by Tricine-SDS-PAGE (16% gel). One gel was fixed and stained with Coomassie Blue. The other gel was blotted to a polyvinylidene difluoride membrane (Millipore) and probed with the anti-Ser^{132} phospho-SmAV antibody.

Protein Phosphorylation—N-SmAV fragments (1 μg each) were phosphorylated in the presence of recombinant ERK/constitutively active MEK protein in a reaction buffer containing 10 mM HEPES, pH 8.0, 100 μM ATP, 10 mM $MgCl_2$, 0.5 mM benzamidine, 1 mM DTT, and 10 μCi of [γ-^{32}P[ATP. The reaction was incubated at 30 °C for 1 h and stopped by adding SDS-PAGE loading buffer.

Mass Spectrometry—Excised one-dimensional bands were subjected to in-gel reduction, alkylation, and enzymatic digestion (Roche Applied Science) in a HEPA-filtered hood to reduce keratin background. LC/MS/MS analysis was performed on the in-gel digest extracts using an Agilent (Santa Clara, CA) 1100 binary pump directly coupled to a mass spectrometer. 8 μl of sample were injected on the column using a LC Packings (Sunnyvale, CA) FAMOS autosampler. Nanobore electrospray columns were constructed from 360-μm outer diameter, 75-μm inner diameter fused silica capillary with the column tip tapered to a 15-μm opening (New Objective, Woburn, MA). The columns were packed with 200 Å 5-μm C18 beads (Michrom BioResources, Auburn, CA), a reverse-phase packing material, to a length of 10 cm. The flow through the column was split precolumn to achieve a flow rate of 350 nl/min. The mobile phase used for gradient elution consisted of (*a*) 0.3% acetic acid, 99.7% water and (*b*) 0.3% acetic acid, 99.7% acetonitrile. LC/MS/MS spectra were acquired on a Thermo LTQ ion trap mass spectrometer (Thermo Corp., San Jose, CA). Needle voltage was set to 3 kV, isolation width was 3 Da, relative collision energy was 30%, and dynamic exclusion was used to exclude recurring ions. Ion signals above a predetermined threshold automatically triggered the instrument to switch

from MS to MS/MS mode for generating fragmentation spectra. The MS/MS spectra were searched against the NCBI nonredundant protein sequence data base using the SEQUEST computer algorithm (12) to produce a list of proteins identified in each sample. Based on the results of the initial LC/MS/MS analysis, the peptides observed that included that site of suspected phosphorylation were targeted in a subsequent LC/MS/MS analysis. The YGIALDSEADSEpSPSRY phosphorylated peptide was targeted and found to be phosphorylated upon manual examination of the MS/MS spectra in comparison with the theoretical MS/MS fragmentation of this phosphopeptide sequence.

Statistical Analysis—All of the values in the text are the means ± S.E. The differences between means were evaluated using a two-tailed Student's *t* test. Significant differences were taken at the $p < 0.05$ level.

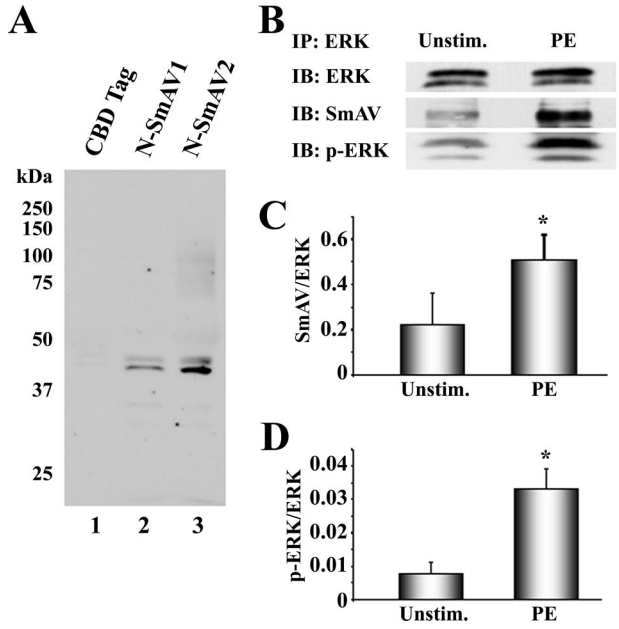

FIGURE 1. **SmAV interacts with ERK1/2.** *A*, immunoblot of N-SmAV1 and N-SmAV2 pulldown samples detected with anti-ERK antibody. *B*, immunoblot (*IB*) of immunoprecipitated (*IP*) proteins from unstimulated and PE-stimulated tissue homogenates as detected by specific antibodies indicated at the *left*. *C*, SmAV densitometry normalized by total ERK densitometry of immunoprecipitates from unstimulated and PE-stimulated conditions. *D*, phospho-ERK densitometry normalized by total ERK densitometry of immunoprecipitates from unstimulated and PE-stimulated samples ($n = 4$).

RESULTS

SmAV Interacts with Two ERK Domains—We have previously predicted, based on sequence analysis, that SmAV contains 2 ERK-binding domains (7), one at residue 219 and a second at residue 774. To determine whether either or both of these predicted sites bind ERK, two N-terminal fragments were expressed as recombinant fragments with N-terminal chitin-binding domain tags. Residues 1–445, containing the first predicted ERK-binding domain, is referred to as N-SmAV1, and residues 446–1250, containing the second predicted ERK-binding domain, is referred to as N-SmAV2.

Initial pulldown experiments using N-SmAV1 or N-SmAV2 as bait and aorta tissue homogenates as prey (Fig. 1*A*) demonstrated that both ERK1 and ERK2 associate with both N-SmAV1 and N-SmAV2. As a negative control, the chitin-binding domain was also expressed separately and used as bait, and as can be seen in Fig. 1*A*, it does not bind detectable ERK.

The interaction between ERK and full-length, endogenous SmAV was confirmed by IP experiments (Fig. 1, *B–D*). Unstimulated aorta tissue homogenates and homogenates of aorta tissue quick frozen in the presence of the α-agonist phenylephrine (PE) were immunoprecipitated with an anti-ERK agarose conjugate. The immunoprecipitates were probed with an anti-ERK antibody (Cell Signaling) in immunoblots. As shown in raw blot (Fig. 1*B*, *top panel*), roughly equivalent amounts of ERK are immunoprecipitated by the ERK antibody from the two sets of homogenates, but significantly more SmAV (*middle panel*) was pulled down from the tissues quick frozen in the presence of PE than in absence of PE. The average densitometry results from three experiments are shown in Fig. 1*C*. We have previously reported that PE increases ERK phosphorylation in this tissue (13), and thus, as expected, more of the ERK pulled down is phosphorylated in the PE-stimulated samples. These results were repeated in three experiments, and the average densitometry was quantitated. The results normalized to total ERK are shown in Fig. 1*D*.

Interaction of SmAV1 with ERK Is Stimulus-dependent—To quantitate the association of ERK with each of the binding sites on N-SmAV1 and N-SmAV2 in the presence of a stimulus, densitometry on pulldown assays was performed with the two expressed N-terminal fragments as bait and homogenates of unstimulated or stimulated aorta tissue as prey. As is seen in Fig. 2*A*, significantly more ERK1 is pulled down with SmAV from the samples activated with PE. This is true for both N-SmAV1 and N-SmAV2. Thus, activation of an α-adrenergic receptor signaling pathway triggers an association of ERK with SmAV. Additionally, when the data are expressed as percentages of the densitometry from

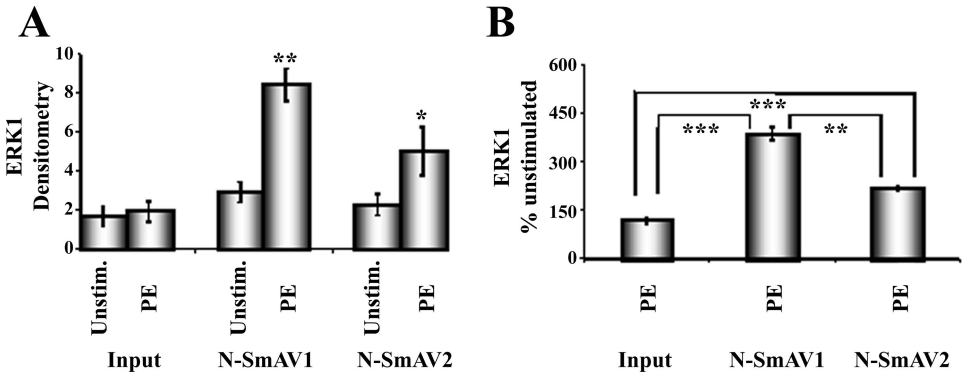

FIGURE 2. **Association of ERK with SmAV is stimulus-specific and domain-specific.** *A*, densitometry of ERK1 immunoblots of N-SmAV1 and N-SmAV2 pulldown samples quick frozen under unstimulated and PE-stimulated conditions. Input signals are included to demonstrate relatively equal pulldown of ERK1. *B*, same data as shown in *A*, but data obtained in the presence of PE are now expressed as percentages of the values from the unstimulated samples ($n = 2$).

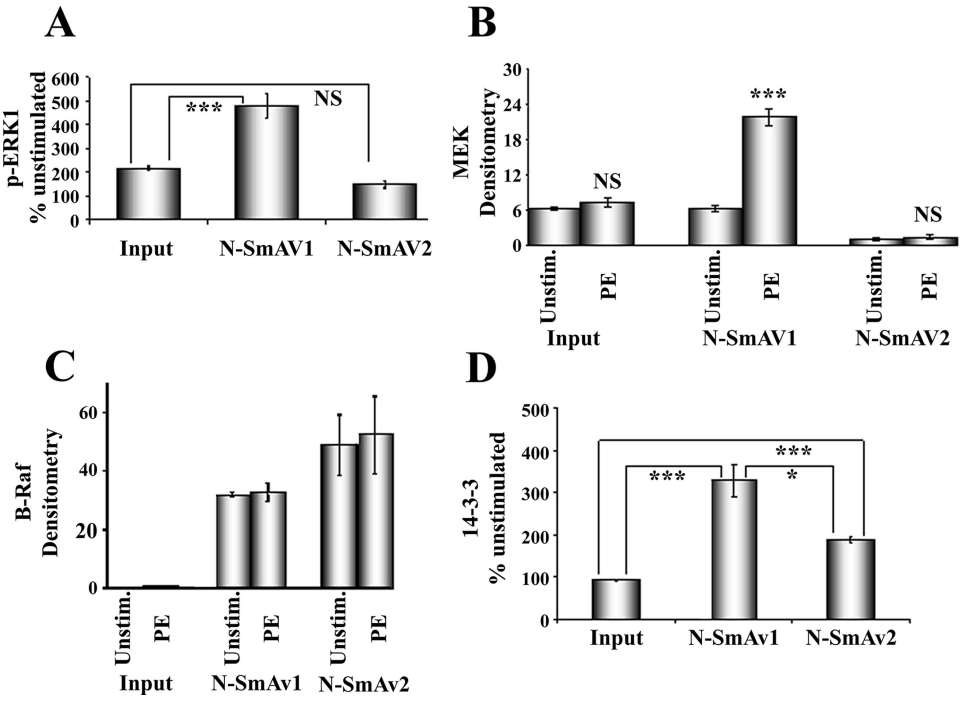

FIGURE 3. **Upstream activators of ERK associate with SmAV.** *A*, N-SmAV1 and N-SmAV2 pulldown samples from homogenates of tissues frozen in the presence or absence of PE, probed for phospho-ERK content. Densitometry expressed as stimulated values as percentages of unstimulated values. *B*, N-SmAV1 and N-SmAV2 pulldown samples from homogenates of tissues frozen in the presence or absence of PE, probed for MEK content. *C*, N-SmAV1 and N-SmAV2 pulldown samples from homogenates of tissues frozen in the presence or absence of PE, probed for B-Raf. *D*, N-SmAV1 and N-SmAV2 pulldown samples from homogenates of tissues frozen in the presence or absence of PE, probed for 14-3-3. The values are expressed as the densitometry values for stimulated samples as percentages of that for unstimulated samples ($n = 3–4$).

the unstimulated sample, it can be seen that the fold increase in ERK1 densitometry associated with N-SmAV1 is significantly greater than that for N-SmAV2 (Fig. 2*B*). The data are shown with respect to ERK1, but similar results were obtained with respect to ERK2 (data not shown).

Phospho-ERK Interacts Preferentially with N-SmAV—Our preliminary results with IP experiments (Fig. 1*D*) indicated that more phospho-ERK was present in PE-stimulated SmAV IP samples than unstimulated samples. This could either be simply due to more phospho-ERK in the PE samples or due to SmAV preferentially binding phosphorylated *versus* nonphosphorylated ERK. Probing of the SmAV pulldown samples for phospho-ERK1 and expressing the results as a percentage of that for unstimulated samples demonstrates (Fig. 3*A*) that the levels of phospho-ERK1 bound to N-SmAV1 in the presence of PE are significantly greater than those seen in the input sample and also greater than those bound to N-SmAV2. Thus, phospho-ERK is concentrated on N-SmAV1.

N-SmAV Binds Upstream Proteins in the MAPK Pathway—The association of phosphorylated ERK specifically with N-SmAV1 raises the question of whether upstream activators of ERK might also be present in the macromolecular complex pulled down with N-SmAV1. The immediate upstream activator of ERK is MEK (MAPK kinase); thus, we probed the pulldown samples for MEK. Interestingly, there is no significant increase in the interaction of N-SmAV2 with MEK in PE-stimulated samples, and in fact, relative to the input signals, almost undetectable levels of MEK bind SmAV2. In contrast, there is a highly significant increase in the interaction of SmAV1 with MEK in PE-stimulated samples (Fig. 3*B*).

Because Raf is the upstream MEKK in most ERK signaling modules, we also probed the pulldown samples for B-Raf. Preliminary immunoblots of tissue homogenates demonstrated no detectable Raf-A or Raf-C in these tissues, and even B-Raf was not abundant and difficult to detect. As can be seen in Fig. 3*C*, however, pulldown with N-SmAV concentrates B-Raf, compared with the levels in the input sample. No stimulus-dependent change in B-Raf binding was seen for either N-SmAV1 or N-SmAV2, thus the binding is constitutive.

Initial sequence analysis of SmAV predicted for a 14-3-3-binding site within N-SmAV2. Because it is known that 14-3-3 interacts with phospho-Raf and promotes binding of regulatory proteins in signaling complexes (14, 15), we also probed the pulldown samples by immunoblot with an antibody specific for 14-3-3. PE stimulation of aorta tissue significantly increases 14-3-3 interaction with both SmAV1 and SmAV2, but the PE-induced fold increase is significantly greater for SmAV1 than SmAV2 (Fig. 3*D*). Thus, the association of phospho-ERK, MEK, B-Raf, and 14-3-3 with SmAV1 demonstrates the formation of a macromolecular signaling complex with N-SmAV1, containing the major members of the ERK signaling module.

A Depolarizing Stimulus Is Less Effective than PE in Causing Association of ERK Signaling Partners with N-SmAV—A depolarizing stimulus is of interest because we have previously shown that depolarization also leads to ERK activation in this tissue but through a different signaling pathway. In the presence of PE, activated ERK uses the actin-binding protein caldesmon as the terminal substrate, whereas in the presence of KCl PSS to depolarize the tissue, activated ERK uses myosin light chain kinase as the substrate (16).

When pulldown experiments are carried out with samples frozen in the presence or absence of KCl PSS to depolarize the tissue, an association of ERK with SmAV can be detected, but in this case ERK associates equally with N-SmAV1 and N-SmAV2 (Fig. 4*A*), and furthermore, the fold change in ERK association upon tissue stimulation with KCl PSS is less than that seen with PE (compare Fig. 2*A*), about 2-fold *versus* 4-fold.

For comparison with the PE stimulation data, we also probed the pulldown samples from tissue stimulated with KCl PSS for binding to phospho-ERK, MEK, and 14-3-3. Binding of phospho-ERK1 and MEK to SmAV1 was seen (Fig. 4, *B* and *C*) but note that the fold increase with KCl PSS stimulation is less than that for PE stimulation. 14-3-3 binding to N-SmAV actually

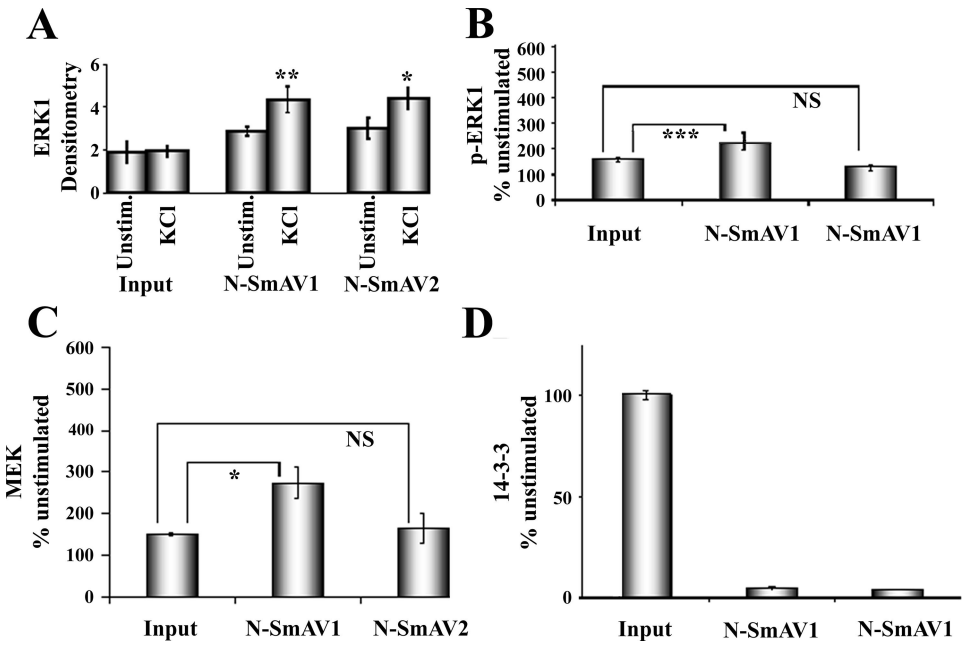

FIGURE 4. **Activation of ERK by depolarization of smooth muscle tissue causes less SmAV binding of ERK signaling module.** *A*, N-SmAV1 and N-SmAV2 pulldown samples from homogenates of tissues frozen in the presence or absence of depolarizing buffer (KCl PSS) and probed for ERK1 content. *B*, N-SmAV1 and N-SmAV2 pulldown samples from homogenates of tissues frozen in the presence or absence of KCl PSS and probed for phospho-ERK1. The results are expressed as the densitometry values for stimulated samples as percentages of that for unstimulated samples. *C*, N-SmAV1 and N-SmAV2 pulldown samples from homogenates of tissues frozen in the presence or absence of KCl PSS and probed for MEK. The results are expressed as the densitometry values for stimulated samples as a percentages of that for unstimulated samples. *D*, N-SmAV1 and N-SmAV2 pulldown samples from homogenates of tissues frozen in the presence or absence of KCl PSS and probed for 14-3-3. The results are expressed as the densitometry values for stimulated samples as percentages of that for unstimulated samples ($n = 3–4$).

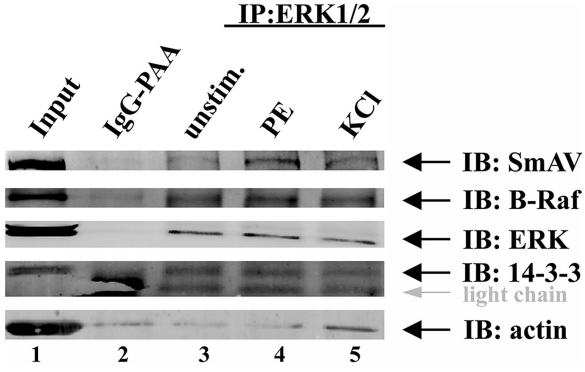

FIGURE 5. **ERK associates with SmAV, B-Raf, and 14-3-3 *in vivo*.** Unstimulated (*lane 3*), PE-stimulated (*lane 4*), or KCl-depolarized (*lane 5*) aorta tissue samples were subjected to immunoprecipitation to an anti-ERK1/2-agarose conjugate. As control, IgG-conjugated agarose beads were used (*lane 2*). An input sample was loaded in *lane 1*. The Western blot was probed for SmAV, B-Raf, ERK, 14-3-3, and actin. *IB*, immunoblot.

decreased relative to input with KCl PSS stimulation rather than the increase seen with PE stimulation. Thus, the mode of interaction of SmAV with ERK signaling partners is stimulus-dependent.

To corroborate the findings from the pulldown assays *in vivo*, we performed an anti-ERK immunoprecipitation with unstimulated, PE-stimulated or KCl PSS depolarized (KCl) aorta tissue. Staining of the immunoprecipitates with specific antibodies against SmAV, B-Raf, ERK, and 14-3-3 demonstrates that all proteins co-precipitate specifically with ERK, because they are not detectable in the negative control (Fig. 5). It can also be ruled out that the proteins unspecifically co-precipitate with actin filaments, because there is the same amount of actin bound to ERK-coupled beads and control beads, at least in the presence of PE. As expected from our *in vitro* pulldown experiments, Raf-B binds constitutively to the signaling complex. In contrast to our previous findings, 14-3-3 also seems to associate constitutively with the ERK-SmAV complex. It is possible that in the ERK immunoprecipitation, 14-3-3 is indirectly pulled down by its association with B-Raf, whereas in the SmAV pulldown, 14-3-3 may directly associate with SmAV. We were not able to detect MEK in the immunoprecipitates, because it runs about the same size as the heavy chain of the ERK antibody used for immunoprecipitation, and the MEK antibody was relatively weakly reacting. Our results furthermore confirm that higher amounts of SmAV co-precipitate together with ERK in PE-stimulated *versus* KCl-depolarized tissue.

ERK Phosphorylates N-SmAV1 but Not N-SmAV2—Analysis of the SmAV sequence predicts for a proline-directed kinase (such as ERK) phosphorylation site to be present adjacent to the predicted ERK-binding site in SmAV1 (7). Thus, the question arises as to whether the activated ERK1/2 bound to SmAV1 might use SmAV itself as a substrate. We have previously reported in cellular imaging studies from this tissue that after PE-mediated ERK activation in the cell cortex, ERK leaves the cortex and translocates to the contractile filament bundles in the cell core to colocalize with, and phosphorylate caldesmon (13). Such a phosphorylation of cortical SmAV may provide a mechanism whereby active ERK1/2 is released from SmAV to be targeted to caldesmon.

Thus, we incubated expressed N-SmAV1 and N-SmAV2 fragments with activated ERK that had been co-expressed with a constitutively active MEK mutant (10) in the presence of [γ-^{32}P]ATP/Mg^{2+}. The products were run in an SDS-PAGE, and the autoradiography results demonstrate that N-SmAV1 but not N-SmAV2 is phosphorylated by activated ERK (Fig. 6*A*). As a positive control, myelin basic protein was also phosphorylated. As a negative control, bovine serum albumin was not phosphorylated under identical conditions (Fig. 6*A*).

Serine 132 of SmAV Is Phosphorylated by ERK—The specific ERK phosphorylation site in N-SmAV1 was identified by phosphorylating SmAV with the expressed ERK in the presence of Mg^{2+}/ATP. The products were run on an SDS-PAGE. The N-SmAV1 band of the Coomassie-stained gel was subjected to

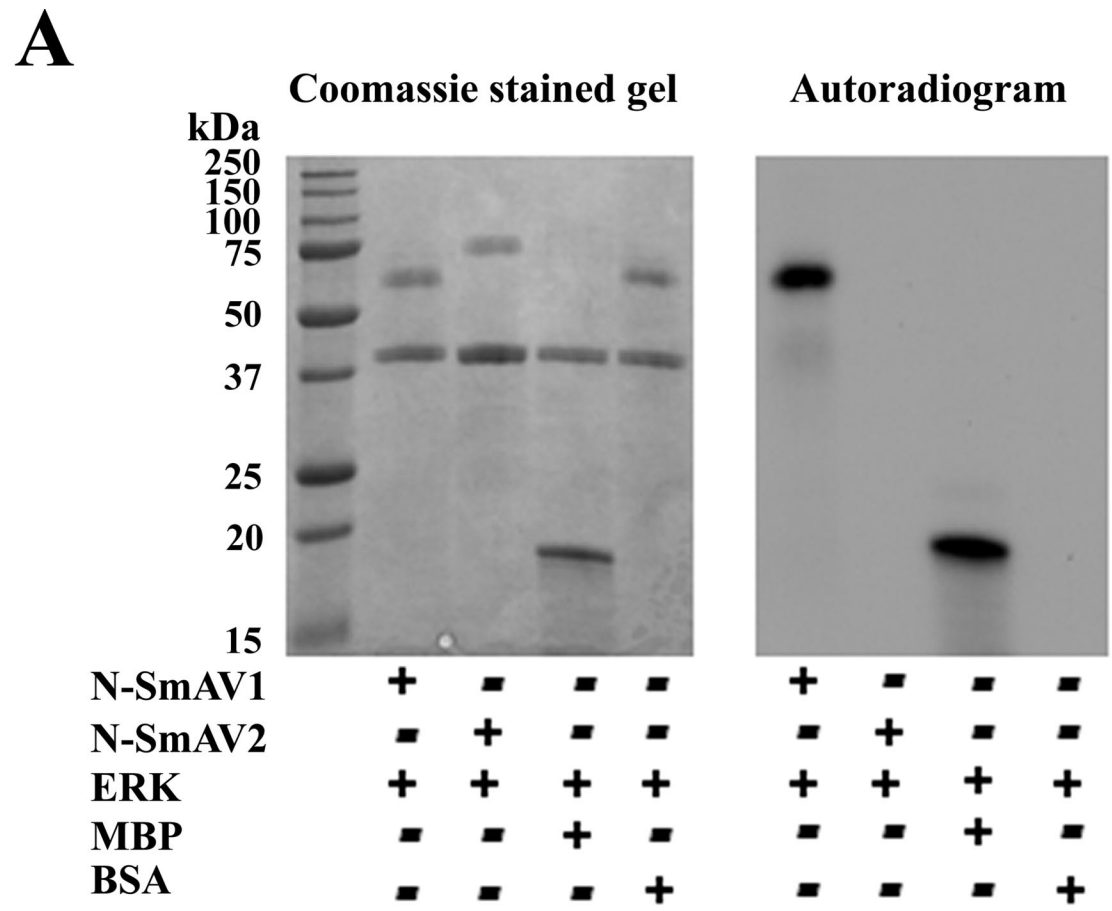
A
Coomassie stained gel
Autoradiogram
kDa
250
150
100
75
50
37
25
20
15
N-SmAV1
N-SmAV2
ERK
MBP
BSA

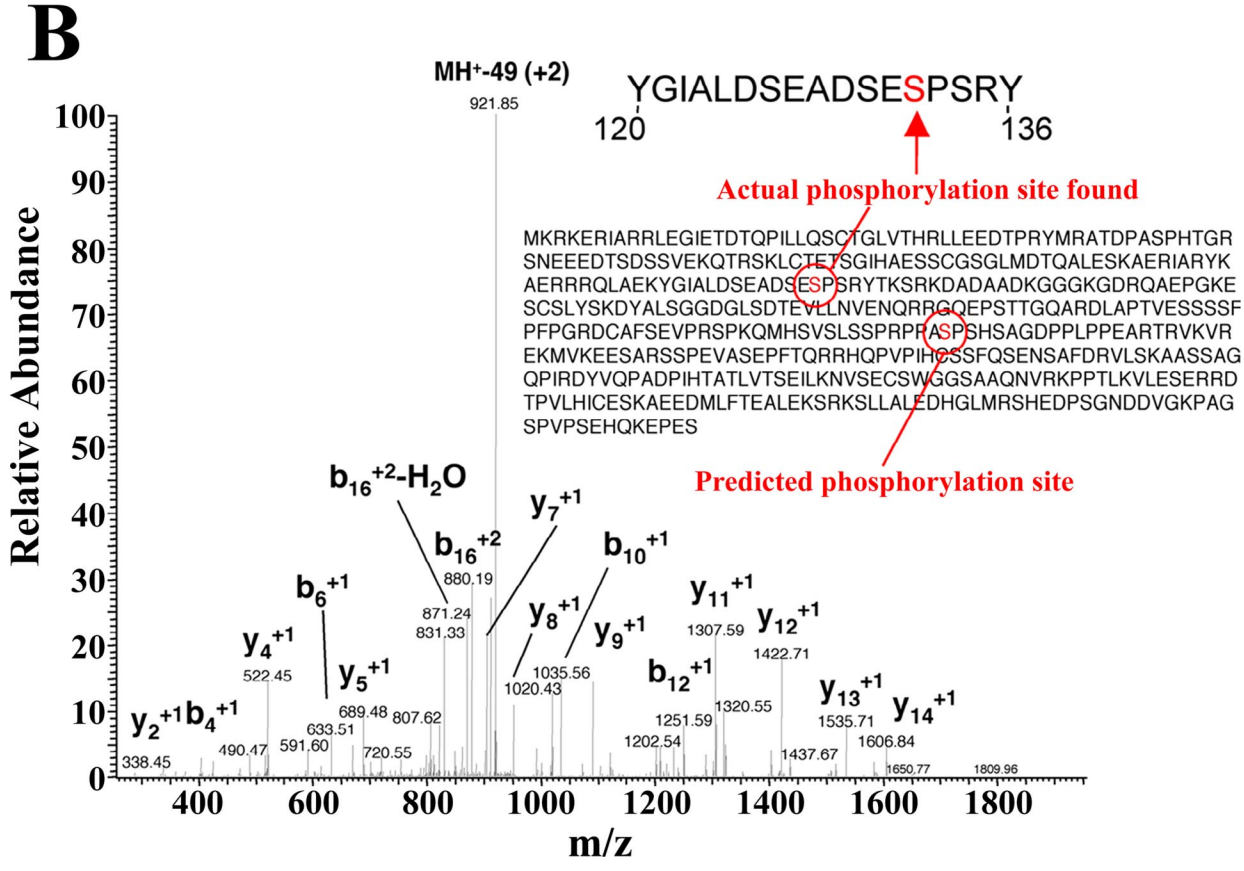
B
MH+-49 (+2)
921.85
YGIALDSEADSESPSRY
120
136
Actual phosphorylation site found
MKRKERIARRLEGIETDTQPILLQSCTGLVTHRLLEEDTPRYMRATDPASPHTGR
SNEEEDTSDSSVEKQTRSKLCTETSGIHAESSCGSGLMDTQALESKAERIARYK
AERRRQLAEKYGIALDSEADSESPSRYTKSRKDADAADKGGGKGDRQAEPGKE
SCSLYSKDYALSGGDGLSDTEVLLNVENQRRGQEPSTTGQARDLAPTVESSSSF
PFPGRDCAFSEVPRSPKQMHSVSLSSPRPFASPSHSAGDPPLPPEARTRVKVR
EKMVKEESARSSPEVASEPFTQRRHQPVPIHCSSFQSENSAFDRVLSKAASSAG
QPIRDYVQPADPIHTATLVTSEILKNVSECSWGGSAAQNVRKPPTLKVLESERRD
TPVLHICESKAEEDMLFTEALEKSRKSLLALEDHGLMRSHEDPSGNDDVGKPAG
SPVPSEHQKEPES
Predicted phosphorylation site
Relative Abundance
m/z
100
90
80
70
60
50
40
30
20
10
0
400
600
800
1000
1200
1400
1600
1800
b_{16}^{+2}-H_2O
b_{16}^{+2}
880.19
871.24
831.33
y_7^{+1}
b_{10}^{+1}
b_6^{+1}
y_4^{+1}
522.45
y_5^{+1}
689.48
633.51
591.60
490.47
338.45
$y_2^{+1}b_4^{+1}$
807.62
720.55
y_8^{+1}
y_9^{+1}
1035.56
1020.43
b_{12}^{+1}
1251.59
1202.54
y_{11}^{+1}
1307.59
y_{12}^{+1}
1422.71
1320.55
y_{13}^{+1}
1535.71
y_{14}^{+1}
1606.84
1437.67
1650.77
1809.96

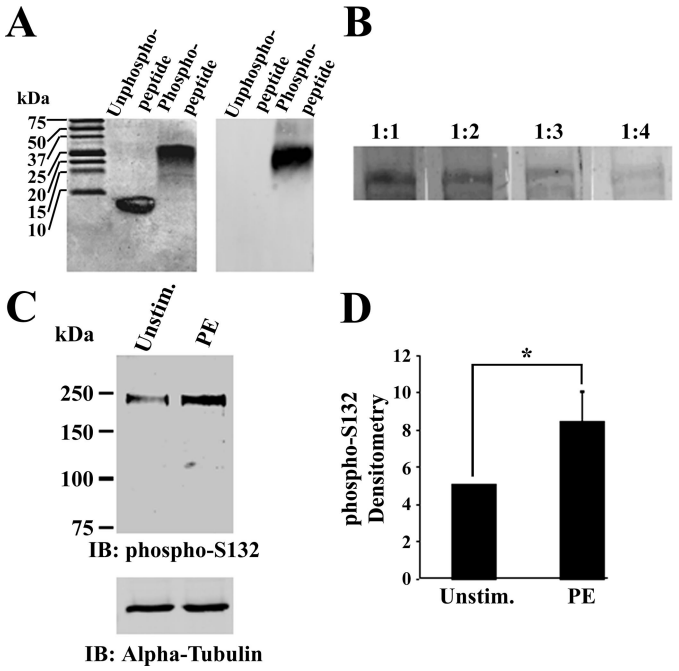

FIGURE 7. **Ser^{132} of SmAV is phosphorylated in smooth muscle tissue in the presence of an α-agonist.** *A*, *left panel*, Coomassie-stained gel of un-phospho- and phospho-peptide as indicated. The slower mobility of the phospho-peptide is because of its octavalent state (see "Experimental Procedures"). Molecular mass standards are show at the *left*. *Right panel*, immunoblot (*IB*) of un-phospho- and phospho-peptide (as indicated) probed with anti-Ser(P)^{132} antibody. *B*, immunoblot of aorta tissue whole cell homogenate probed with anti-Ser(P)^{132} antibody in the presence of antigen (peptide) with the antibody:antigen ratio indicated at the *top*. *C*, *upper panel*, immunoblot of aorta tissue whole cell homogenates, probed with anti-Ser(P)^{132} antibody, demonstrating specificity relative to other proteins in homogenate as well as stimulus dependence of signal. *Lower panel*, immunodetection of α-tubulin to confirm equal lane loading. *D*, densitometry for SmAV Ser^{132} phosphorylation in aorta tissue samples quick frozen under the indicated conditions ($n = 3$).

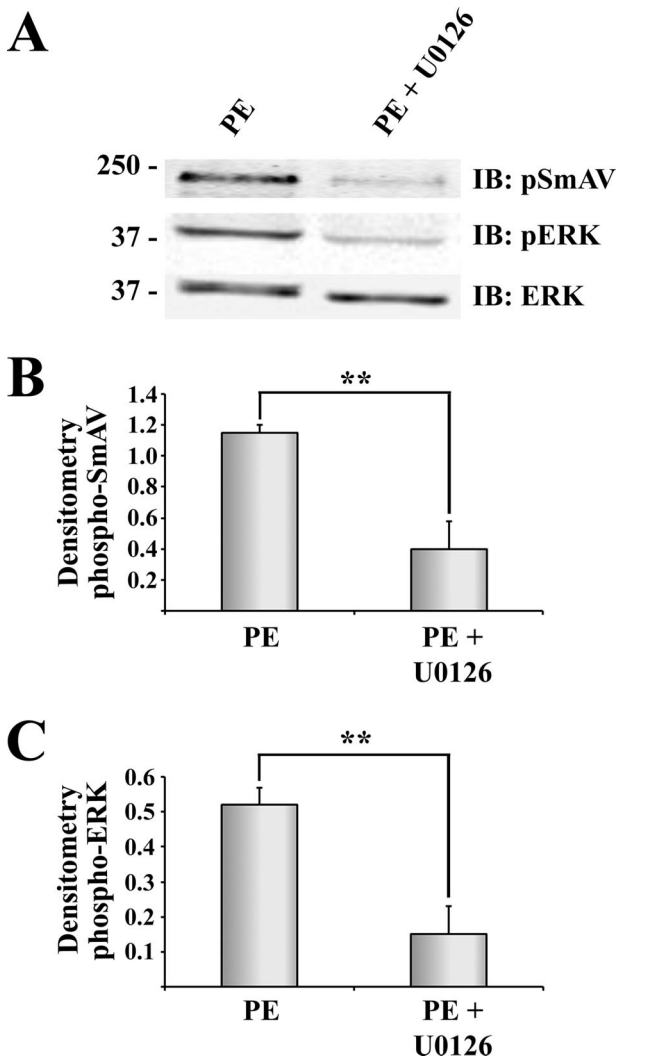

FIGURE 8. **A MEK inhibitor blocks PE-induced SmAV Ser^{132} phosphorylation.** *A*, aorta tissue was pretreated either with the MEK inhibitor U0126 or Me_2SO as control, prior to PE stimulation. The homogenates were subjected to SDS-PAGE and subsequent Western blotting. The membrane was probed for phospho-SmAV Ser^{132}, ERK, and phospho-ERK. *B*, densitometry of phospho-SmAV. *C*, densitometry of phospho-ERK ($n = 3$). *IB*, immunoblot.

mass spectrometry analysis for the detection of phospho-sites (Fig. 6*B*). It was determined that the actual phosphorylation site was not at residue Ser^{248} as predicted by sequence analysis but actually at an upstream site with a similar consensus sequence, Ser^{132}.

SmAV Is Phosphorylated by ERK at Ser^{132} in Smooth Muscle Tissue—To check the functional relevance of the phosphorylation of SmAV Ser^{132}, we raised a phospho-specific antibody to this site. A multivalent antigenic peptide was synthesized from a SmAV sequence surrounding the phosphorylated Ser^{132} (see "Experimental Procedures"). The Ser(P)^{132} peptide was used to raise a rabbit polyclonal phospho-specific antibody. An unphosphorylated peptide was also synthesized for control experiments. The specificity of the antibody was tested by immunoblot of phospho- and nonphosphorylated peptides on a 16% Tricine gel. The Coomassie-stained gel (Fig. 7*A*, *left panel*) shows the difference in mobility between the multivalent phosphopeptide and the univalent nonphosphopeptide peptides. No cross-reactivity is seen on immunoblot of the nonphosphorylated peptide with the phospho-antibody (Fig. 7*A*, *right panel*). Additionally, as shown in Fig. 7*B*, binding of the antibody to phosphorylated SmAV in vascular tissue homogenates can be competed away by the addition of increasing amounts of the antigen.

Using this antibody in immunoblots against vascular tissue homogenates, we saw significantly higher levels of antibody

FIGURE 6. **ERK phosphorylates SmAV at Ser^{132} *in vitro*.** *A*, N-SmAV1 but not N-SmAV2 is phosphorylated *in vitro* by activated ERK/MEK. The *left panel is* a Coomassie-stained gel of an electrophoresed reaction mixture as indicated below the gel. Molecular mass standards are indicated at the *left*. The *right panel* is the autoradiogram of the same dried gel. *B*, MS/MS spectrum of the phosphorylation peptide with sequence YGIALDSEADSEpSPSRY. The doubly charged precursor ($[M+2H]^{+2}$) was observed with a mass of 970.5 Da and includes the phosphorylation post-translational modification. The neutral loss of phosphoric acid from the precursor (98-Da loss, observed as a 49-Da loss from precursor for a doubly charged peptide) is characteristic of MS/MS fragmentation of phosphopeptides and was observed at 921.85 Da. The predicted phosphorylation site was on the Ser^{248} residue but was actually found on the Ser^{132} residue. Fragment ions y_5, y_7, y_8, y_9, y_{11}, y_{12}, y_{13}, y_{14}, b_{16}, and b_{17} all include the phosphorylated residue and provide evidence of phosphorylation on Ser^{132} (not all labeled in figure for clarity). Furthermore, residues b_{12} and y_4 both do not have the 80 mass shift attributed to addition of phosphate, providing further evidence of phosphorylation on Ser^{132}. *BSA*, bovine serum albumin; *MBP*, myelin basic protein.

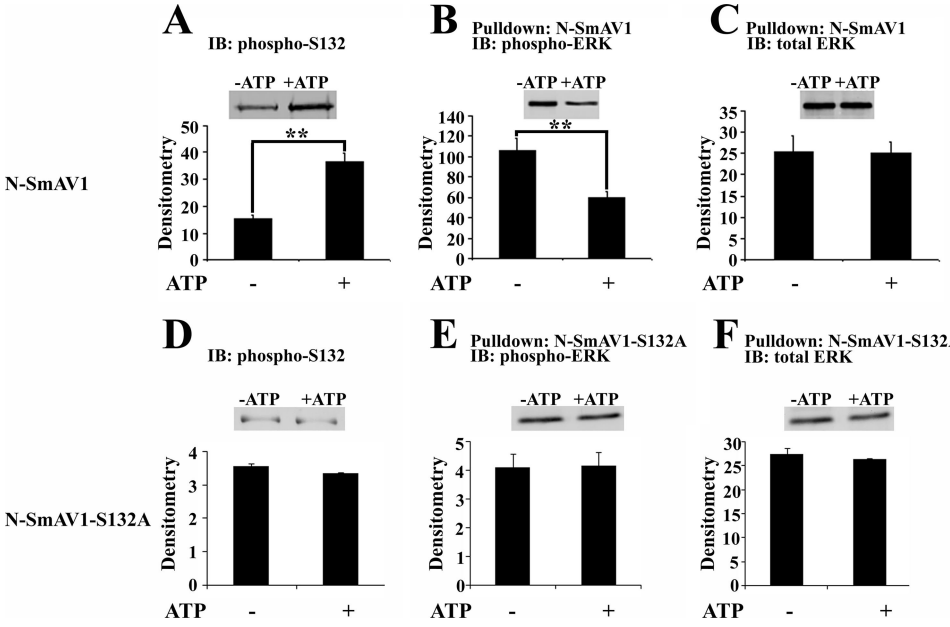

FIGURE 9. **ERK-mediated phosphorylation of SmAV decreases pulldown of phospho-ERK with SmAV.** *A*, immunoblot (*IB*) with Ser(P)^{132}-SmAV antibody of reaction of N-SmAV1 with constitutively active ERK with or without ATP. A typical blot is presented in the *inset*. *B*, pulldown of phospho-ERK with N-SmAV1 in the presence or absence of ATP as indicated, detected with anti-phospho-ERK antibody. *C*, pulldown of recombinant ERK with N-SmAV1 in the presence or absence of ATP as indicated, detected with anti-total ERK antibody. *D*, immunoblot with Ser(P)^{132}-SmAV antibody of reaction of N-SmAV1-S132A with constitutively active ERK with or without ATP. A typical blot is presented in the *inset*. *E*, pulldown of phospho-ERK with N-SmAV1-S132A in the presence or absence of ATP as indicated, detected with anti-phospho-ERK antibody. *F*, pulldown of recombinant ERK with N-SmAV1-S132A in the presence or absence of ATP as indicated, detected with anti-total ERK antibody ($n = 3$).

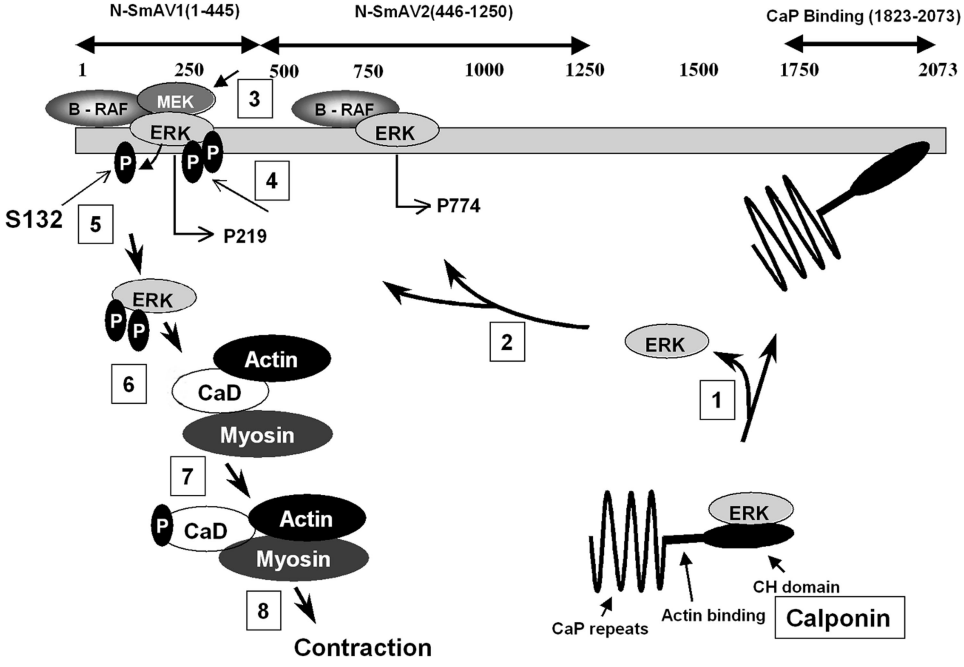

FIGURE 10. **A model of possible function of SmAV as a scaffold protein.** SmAV is represented as a *solid gray bar* with amino acid residue numbers indicated at the *top*. The location of the two predicted ERK-binding sites (based on sequence analysis), p219 and p774, are indicated. SmAV-interacting proteins based on data from this work as well as Leinweber *et al.* (23) are indicated. The sequential flow of events is indicated by *arrows* and *numbers* (*boxed*) as described in the text.

staining in homogenates of tissues quick frozen in the presence of PE than in the absence of the stimulus (Fig. 7*C*). The mean densitometry of the results from three separate experiments similar to that shown in Fig. 7*C* is shown in Fig. 7*D*. Ser^{132} phosphorylation of SmAV is significantly increased with PE stimulation. Preincubation of the tissues, quick frozen in the presence of PE, with the MEK inhibitor U0126 significantly decreased Ser^{132} phosphorylation of SmAV, corroborating the hypothesis that ERK uses SmAV as a substrate (Fig. 8).

Phosphorylation of SmAV at Ser^{132} Decreases the Association with ERK—To test the hypothesis that phosphorylation of SmAV by ERK at Ser^{132} decreases the association between the proteins, we performed an *in vitro* experiment where we controlled the phosphorylation of SmAV by activated ERK by combining the recombinant proteins in the presence or absence of ATP. The combination of SmAV and ERK in the presence of ATP causes phosphorylation of SmAV and actually a decrease in the amount of p-ERK pulled down with SmAV compared with that obtained in the absence of ATP. This effect was not visible with a SmAV mutant where the ERK phosphorylation site Ser^{132} is replaced by alanine (Fig. 9, *D–F*), indicating that phosphorylation of SmAV at Ser^{132} by ERK decreases the association of phospho-ERK with SmAV.

DISCUSSION

The results presented here, together with past cellular studies from our group (7), demonstrate that SmAV displays properties that allow it to function as an ERK scaffolding protein. Scaffolds have been defined as proteins, generally with no applicable enzymatic activity "that interact with a signaling pathway to create a functional signaling module and to control the specificity of signal transduction" (5). We have previously shown that SmAV knockdown in vascular smooth muscle tissue inhibits ERK activation and contraction induced by the α-agonist PE (7). We demonstrate here that N-terminal SmAV sequence (N-SmAV-1) associates with ERK, MEK, Raf, and 14-3-3, all known members of a classical ERK signaling pathway, in an agonist- and pathway-specific manner. Taken together, these results demonstrate

an ERK scaffolding function for this recently described smooth muscle protein.

Two ERK pathways, targeted to two different ERK substrates have previously been shown to co-exist in the cell type from which SmAV was first identified (17). α-Agonist activation has been shown to lead to ERK activation and subsequent phosphorylation of caldesmon at an ERK phosphorylation site. Phosphorylation at this site has been shown to increase actomyosin ATPase activity (18, 19) and, hence, contractility. In contrast, depolarization-mediated activation leads to activation of calcium-calmodulin-kinase 2 and subsequent activation of ERK, but in this case, ERK activation leads to increased myosin phosphorylation and contractility, presumably via ERK-mediated phosphorylation of myosin light chain kinase. In the present study we showed that α-adrenoreceptor activation of tissues with PE causes a greater fold increase in the association of N-SmAV1 in pulldown experiments with ERK, phospho-ERK, MEK, and 14-3-3 than does depolarization of tissues even though both modes of stimulation lead to ERK activation. Previously, PE stimulation has been shown to target ERK to the cell surface (8), but depolarization leads to a homogeneous cellular distribution of ERK (20). Interestingly, both SmAV and ERK translocate to the membrane upon PE stimulation at the same time point (4 min) in isolated ferret aorta cells, as has been shown previously (7, 8). The stimulus-specific nature of N-SmAV1 binding to ERK signaling partners could serve to spatially sequester the α-agonist-activated ERK pathway from the depolarization-activated ERK pathway and provide a mechanism whereby ERK in the intracellular environment chooses the signaling pathway to follow in response to a specific agonist.

Multiple cellular studies have demonstrated a biphasic targeting of MAPKs, first from the cytosol to the cell cortex/membrane and, subsequently, either to the nucleus in proliferating cells (21, 22) or to the contractile filaments in differentiated smooth muscle (8). A possible mechanism triggering the release from its cortical targeting has been lacking. We have now shown that ERK, after preferentially associating with N-SmAV1 and becoming activated, uses N-SmAV1 as a substrate and phosphorylates (*in vitro* and *in vivo*) N-SmAV1 at Ser^{132}. We have also shown that ERK-mediated phosphorylation of N-SmAV1 decreases the association of active ERK from the scaffold. The release of active ERK then allows the subsequent targeting to the final substrate of ERK. The binding of unphosphorylated ERK to N-SmAV2 may feed substrate to activated MEK associated with N-SmAV1.

Leinweber *et al.* (23) showed that the ERK-binding domain of calponin is the N-terminal calponin homology domain, which Gangopadhyay *et al.* (7) showed is the domain of calponin that binds the C-terminal end of SmAV. These past studies can be combined with the work presented here in a model shown in Fig. 10, whereby (*a*) ERK, bound to the calponin homology domain of calponin, colocalizes with SmAV in the cell cortex (7), and binding of the calponin homology domain to SmAV 1823–2073 releases ERK. (*b*) ERK binds the two ERK-binding sites in the N-terminal portion of SmAV. (*c*) MEK is recruited to SmAV and activated by B-Raf. (*d*) ERK is phosphorylated and activated by MEK. (*e*) Activated ERK phosphorylates Ser^{132} of SmAV, and phosphorylation of SmAV may cause a conformational change in the SmAV molecule or the charge difference may repel ERK from SmAV, releasing phospho-ERK. (*f*) phospho-ERK associates with and phosphorylates caldesmon. (*g*) Phosphorylation of caldesmon makes the actin available for the interaction with myosin, which in turn increases contractility. In summary, we have shown that SmAV displays the properties necessary to function as an ERK scaffold, creating a functional signaling module that can control the stimulus specificity of signal transduction.

Acknowledgment—We thank Dr. Melanie H. Cobb (University of Texas Southwestern Medical Center, Dallas, TX) for providing the ERK construct.

REFERENCES

1. Chuderland, D., and Seger, R. (2005) *Mol. Biotechnol.* **29,** 57–74
2. Pullikuth, A. K., and Catling, A. D. (2007) *Cell Signal.* **19,** 1621–1632
3. Morgan, K. G., and Gangopadhyay, S. S. (2001) *J. Appl. Physiol.* **91,** 953–962
4. Taggart, M. J., and Morgan, K. G. (2007) *Semin. Cell Dev. Biol.* **18,** 296–304
5. Morrison, D. K., and Davis, R. J. (2003) *Annu. Rev. Cell Dev. Biol.* **19,** 91–118
6. Dhillon, A. S., and Kolch, W. (2002) *Arch. Biochem. Biophys.* **404,** 3–9
7. Gangopadhyay, S. S., Takizawa, N., Gallant, C., Barber, A. L., Je, H. D., Smith, T. C., Luna, E. J., and Morgan, K. G. (2004) *J. Cell Sci.* **117,** 5043–5057
8. Khalil, R. A., and Morgan, K. G. (1993) *Am. J. Physiol. Cell Physiol.* **265,** C406–411
9. Menice, C. B., Hulvershorn, J., Adam, L. P., Wang, C. A., and Morgan, K. G. (1997) *J. Biol. Chem.* **272,** 25157–25161
10. Robbins, D. J., Zhen, E., Owaki, H., Vanderbilt, C. A., Ebert, D., Geppert, T. D., and Cobb, M. H. (1993) *J. Biol. Chem.* **268,** 5097–5106
11. Veprek, P., and Jezek, J. (1999) *J. Pept. Sci.* **5,** 203–220
12. Yates, J. R., 3rd, Eng, J. K., McCormack, A. L., and Schieltz, D. (1995) *Anal. Chem.* **67,** 1426–1436
13. Khalil, R. A., Menice, C. B., Wang, C. L., and Morgan, K. G. (1995) *Circ. Res.* **76,** 1101–1108
14. Petosa, C., Masters, S. C., Bankston, L. A., Pohl, J., Wang, B., Fu, H., and Liddington, R. C. (1998) *J. Biol. Chem.* **273,** 16305–16310
15. Michaud, N. R., Fabian, J. R., Mathes, K. D., and Morrison, D. K. (1995) *Mol. Cell. Biol.* **15,** 3390–3397
16. Abraham, S. T., Benscoter, H. A., Schworer, C. M., and Singer, H. A. (1997) *Circulation Res.* **81,** 575–584
17. Wier, W. G., and Morgan, K. G. (2003) *Rev. Physiol. Biochem. Pharmacol.* **150,** 91–139
18. Gerthoffer, W. T., Yamboliev, I. A., Shearer, M., Pohl, J., Haynes, R., Dang, S., Sato, K., and Sellers, J. R. (1996) *J. Physiol.* **495,** 597–609
19. Adam, L. P., Franklin, M. T., Raff, G. J., and Hathaway, D. R. (1995) *Circ. Res.* **76,** 183–190
20. Marganski, W. A., Gangopadhyay, S. S., Je, H. D., Gallant, C., and Morgan, K. G. (2005) *Circ. Res.* **97,** 541–549
21. Pouysségur, J., and Lenormand, P. (2003) *Eur. J. Biochem.* **270,** 3291–3299
22. Gonzalez, F. A., Seth, A., Raden, D. L., Bowman, D. S., Fay, F. S., and Davis, R. J. (1993) *J. Cell Biol.* **122,** 1089–1101
23. Leinweber, B. D., Leavis, P. C., Grabarek, Z., Wang, C. L., and Morgan, K. G. (1999) *Biochem. J.* **344,** 117–123